Simulation of a SOFC/Battery powered vehicle

Bessékon, Yannick; Zielke, Philipp; Wulff, Anders Christian; Hagen, Anke

Published in:
International Journal of Hydrogen Energy

Link to article, DOI:
10.1016/j.ijhydene.2018.11.126

Publication date:
2019

Document Version
Peer reviewed version

Simulation of a SOFC/Battery powered vehicle

Yannick Bessekon [a], Philipp Zielke [b], Anders C. Wulff [b], and Anke Hagen [b*]

[a]Carl von Ossietzky University, Ammerländer Heerstrasse 114, 26129 Oldenburg, Germany

[b]DTU Energy, Frederiksborgvej 399, 4000 Roskilde, Denmark

[*] anke@dtu.dk, +45 46775884, corresponding author

Abstract (150 words)

Solid oxide fuel cells (SOFCs) have received attention in the transport sector for use as auxiliary power units or range extenders, due to the high electrical efficiency and fuelling options using existing fuel infra structure. The present work proposes an SOFC/battery powered vehicle using compressed natural gas (CNG), liquefied natural gas (LNG) or liquefied petroleum gas (LPG) as fuels. A model was developed integrating an SOFC into a modified Nissan Leaf Acenta electrical vehicle and considering standardized driving cycles. A 30 liter fuel tank and 12 kW SOFC module was simulated, including a partial oxidation fuel reformer. The results show a significant increase of the driving range when combining the battery vehicle with an SOFC. Ranges of 264 km, 705 km and 823 km using respectively CNG, LNG and LPG compared to 170 km performed by the original vehicle were calculated. Furthermore, a thorough sensitivity analysis was carried out.

Keywords

SOFC, fuel cell, BEV, hydrocarbon fuel, driving range

1. Introduction

In order to reduce global CO_2 emissions, alternatives to internal combustion engines have to be deployed in the transportation sector. One of those alternatives are battery electrical vehicles (BEVs), which are more efficient and less energy consuming than internal combustion engine (ICE) vehicles 1. More importantly, they have the option of using renewable energy sources as primary fuels, i.e. the processes for electricity production. However, one of the main technological challenges of such vehicles is the energy storage density using current battery technologies, which limits their driving ranges as compared to ICE vehicles [2]. Furthermore, long charging times are still inconvenient for the users. A solution could be the hybridization using fuel cells. Polymer electrolyte fuel cells (PEFC) have been considered for some time in the transport sector with the advantage of their low weight and their relatively fast start-up process. However, the challenges of high costs due to use of noble metals and the need for production and storage of the hydrogen fuel limit their widespread introduction and applications [3]. Both, the battery and PEFC based vehicles still have the challenge of insufficient distribution of charging/fuelling stations needed for a full coverage, which require high investment (and maintenance) costs.

Solid oxide fuel cells (SOFC) have gained interest in the transport sector more recently. SOFCs combine high electrical efficiency with the option of choosing between various readily available high density fuels, which can extend the range of the purely BEVs on one side and can make use of the existing fuelling infrastructure on the other [4. So far, SOFCs have been considered as auxiliary power units (APU) and range extenders in the transport sector [5, 6, 7, 8]. These concepts can significantly increase the performances of the vehicle and take advantage of the current fuel

infrastructure (e.g. compressed natural gas), which significantly reduces costs for introducing a vehicle fleet and fuel distribution and storage. Additionally, SOFCs have a higher electrical efficiency and potentially lower manufacture cost compared to PEFC [9].

In order to take advantage of the existing fuel infrastructure for transportation in combination with an SOFC vehicle, the availability and distribution of fuelling stations has to be considered, in addition to options for producing these fuels based on renewable energy sources. In table 1, the density of fuelling/charging stations for selected European countries is listed. Apart from petrol for ICE vehicles and chargers for BEVs, compressed natural gas (CNG), liquefied natural gas (LNG), and liquefied petroleum gas (LPG) are listed as potential fuels for SOFCs, and hydrogen (H_2) for PEFCs and SOFCs. Petrol stations have naturally the highest density. In some countries, also a large number of public electrical chargers is available. It has to be noted that the density is an average value, i.e. the distribution of charging and fuelling stations is expected to be higher in densely populated areas such as cities. In contrast to hydrogen filling stations, which are still very scarce, CNG and LPG filling stations are more present in many of the listed countries as shown Table 1.

Table 1. Number of fuelling/charging stations by type of fuel per 100 km^2, from refs. [10, 11, 12, 13]

	Area	Petrol	CNG	LNG	LPG	H_2	Public chargers
	[km^2]	[station/ 100 km^2]	[station/ 100 km^2]	[station/ 100 km^2]	[station/ 100 km^2]	[station/ 100 km^2]	[station/ 100 km^2]
Austria	83871	3.2	0.21	n/a	0.05	0.005	4.388
Denmark	43094	4.7	0.02	n/a	0.01	0.026	0.283
France	640679	1.7	0.01	0.001	0.27	0.002	0.001
Germany	357114	4.1	0.08	0.001	2.02	0.014	2.435
Italy	301336	6.9	0.33	0.003	1.24	0.001	0.027
Netherlands	41850	10.0	0.36	0.053	3.27	0.005	3.673
Spain	505992	2.2	0.01	0.005	0.10	0.001	0.003
UK	242495	3.5	0.01	0.005	0.60	0.006	0.002
Switzerland	41284	8.3	0.33	n/a	0.15	0.012	8.916

In addition to the geographical density of stations, also the fuelling/charging time has to be considered. Table 2 shows the required times for one fuelling/charging cycle. It becomes clear that charging standard plug-in BEVs takes 60 to 80 times longer than fuelling a vehicle with a combustion engine with LPG/LNG or diesel/gasoline, respectively.

Table 2. Fuelling time and theoretical capacity for selected fuels and BEVs, from refs. [14, 15, 16]

	Charge time (minutes)	Max capacity (vehicles /day)

Diesel / gasoline*	6	240
LPG/LNG	8	180
CNG	12	120
H_2 -@70MPa	15	96
Standard plug -In	480	3

*Including heavy duty vehicles

To investigate the effect of SOFC technology for automotive range extension, the current study examines a model integrating an SOFC unit into a commercial Nissan Leaf Acenta BEV using the software MATLAB®. Performances using standard driving cycles and different powertrain configurations were simulated and the obtainable driving ranges calculated. CNG, LPG, and LNG were selected as available fuels. Different control strategies for the fuel cell system were investigated as part of the overall powertrain management. Furthermore variations of the power generation capacities were studied.

2. Methods and concept

2.1 Vehicle model

The first part of this study aimed at establishing a model of an electrical vehicle and a fuel cell unit. The powertrain of the vehicle was divided into several modules (see Figure 1) and translated into MATLAB® scripts to estimate the size of the main components. The main concepts and methods for each submodule are introduced in this section.

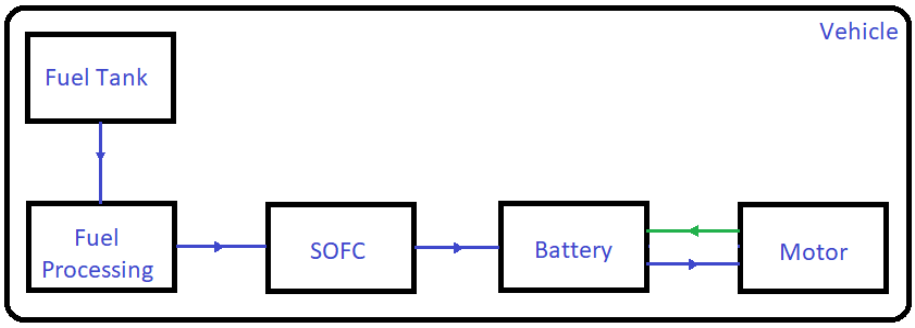

Figure 1 Powertrain flowsheet with submodules

The power of the electric motor (P_{mot}) in case of an acceleration or deceleration is expressed in equation (1), from ref. [17].

$$P_{mot} = \begin{cases} \frac{P_{te}}{\eta_m \eta_g} \ (Acceleration) \\ P_{te} \eta_m \eta_g \eta_{reg} \ (Deceleration) \end{cases} \quad (1)$$

In this equation, P_{te} is the traction power of the vehicle, depending on parameters such as vehicle frontal area, aerodynamic drag coefficient and vehicle speed ([18]), η_m is the motor efficiency, η_g is the gear efficiency and η_{reg} is the share of regenerated power through regenerative breaking.

2.1.1 Battery electrical vehicle (BEV)

The BEV part of the model covered the vehicle's dynamics, the electrical motor, and the lithium ion battery modules. The final objective of the battery modelling is to calculate the maximum driving range according to the data input such as the mechanical parameters, driving cycle and – for the SOFC/BEV - the SOFC stack specifications. The related battery parameter is the depth of discharge (DoD). Other variables such as the battery temperature that plays a significant role for the safety of the overall system are neglected at this stage. The first parameter for the DoD calculations is the internal resistance of the battery. This information is provided by the datasheet of commercial batteries. The second parameter is the open circuit voltage (E_{OCV}). Considering lithium ion batteries (LIBs), equation (2) was used to simulate the E_{OCV} as a function of the state of charge (SoC), where the parameters *a, b, c, d, m,* and *n* depend on the materials of the battery and were taken from Zhang et al. [19]. A $LiMn_2O_4$ (LMO) based battery is considered for the present work.

$$E_{ocv} = a + b(-\ln SoC)^m + cSoC + de^{n(SoC-1)} \quad (2)$$

Based on these values, the current can be calculated in the case of the battery entirely supporting the powertrain, and also when the SOFC module or regenerative power are higher than the load required by the vehicle. The power provided by or supplied to the battery (P_{bat}) is given by equation (3), where P_{ac} is the power of the vehicle's accessories and P_{FC} the electrical power output of the fuel cell module.

$$P_{bat} = P_{mot} + P_{ac} + P_{FC} \quad (3)$$

Once P_{bat} is determined, the value of the current (I) is a solution of the quadratic equations (4), from ref. [20] with R_{eq} being the internal resistance of the battery and E_{OCV} the open circuit voltage:

$$I = \begin{cases} \frac{E_{ocv} - \sqrt{{E_{ocv}}^2 - 4R_{eq}P_{bat}}}{2R_{eq}} (if\ P_{bat} > 0, discharge\ mode) \\ \frac{-E_{ocv} + \sqrt{{E_{ocv}}^2 + 4R_{eq}P_{bat}}}{2R_{eq}} (if\ P_{bat} < 0, charge\ mode) \end{cases} \quad (4)$$

Based on these equations, the new depth of discharge of the battery is computed using the equations (5), from refs. [17], [21].

$$DoD_{Discharge} = \begin{cases} DoD + \frac{1}{3600} * \frac{I^k}{C_p} (If\ P_{bat} > 0, discharge\ mode\ ) \\ DoD - \frac{1}{3600} * \frac{I}{C_p} (If\ P_{bat} < 0, charge\ mode\ ) \end{cases} \quad (5)$$

2.1.2 SOFC unit

The fuels (CNG/LNG/LPG) are converted into hydrogen and carbon monoxide in the external reformer. The purpose of the SOFC module is to convert the chemical energy contained in the carbon monoxide and the hydrogen into electricity. The chemical energy considered for this step is the lower heating value (LHV) of the gas mixture.

The module is composed of a number of individual SOFC stacks. For the present study, a commercial 30-cell stack from the manufacturer SOFCMAN based on the anode supported cell configuration, with a nominal electrical power of 2 kW and a weight of 9 kg was used [22]. The power input to the stack can be derived by increasing this value using the electrical efficiency η_{SOFC}. The basic concept of the module is presented in Figure 2 and equation (6) (from refs. [17, 23]), where P_{FC_in} is the chemical power of the $CO+H_2$ mixture entering the module per second, P_{FC_out} is the electrical power of the FC module, η_{FC_BoP} is the share of electrical energy required by the balance of plant (BoP) and η_{FC_loss} is the part of fuel not processed by the module through partial fuel utilization.

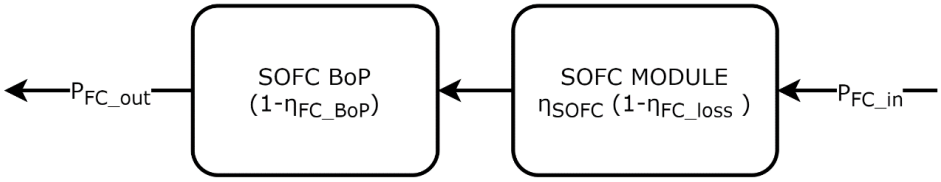

Figure 2. Concept of the SOFC module

$$P_{FC\_in} = \frac{P_{FC\_out}}{\eta_{SOFC}(1-\eta_{FC\_BoP})(1-\eta_{FC\_loss})} \quad (6)$$

Considering eq. (3) and (6), the average electrical power demand of the vehicle is known. To achieve this power, the SOFC module is realized by the combination of several stacks (Nb_{stack}) with the nominal power of $Power_{FCmodel}$. Sufficient power to recharge 50% of the battery's capacity ($Capacity_{battery}$) during a specified charging time (*Charging-time*) is required in addition to the vehicle's average electrical power ($Power_{average}$) calculated on a driving cycle using the BEV mode (see equation (7)).

$$Nb_{stack} = \frac{0.5 * Capacity_{battery}/Charging_{time} + Power_{average}}{Power_{FC_{model}}\left(1-\eta_{FC_{BoP}}\right)} \quad (7)$$

The fuel cell stacks need to be warmed up to the operating temperatures of around 750 ^{o}C before producing electricity. For a first order estimation of the thermal mass ($Q_{FC\_heating}$), the SOFC stacks were considered to be entirely made of Crofer 22 (weight according to the manufacturer), a metal typically used for the SOFC interconnects due to its corresponding thermal expansion coefficient with the other materials of the cells and its corrosion properties at elevated temperatures [24]. It is further assumed that the heating energy can be supplied using an electrical heater. For determining the heating power ($P_{FC\_heating}$) for a specific warm up time ($Time_{FC\_heating}$) equation (8) was used assuming an ideal heat transfer case.

$$P_{FC\_heating} = \frac{Q_{FC\_heating}}{Time_{FC\_heating}} \quad (8)$$

The heating power could also be produced by burning the fuel contained in the tank (number of moles of combusted fuel (Mol_{fuel}), equation (9)). This concept was for example used for heating of SOFC APU [25].

$$Mol_{fuel} = \frac{P_{FC\_heating}}{LHV_{fuel}} \quad (9)$$

2.1.3 Reformer unit

Especially the lower hydrocarbons (e.g. methane) could be reformed directly in the SOFC through internal reforming on the state-of-the-art Ni containing anode, affecting the thermal management of the unit. Steam reforming of methane is an endothermal reaction, leading to local cooling and to large thermal gradients over the stack, which might risk the mechanical integrity of the SOFC stack. In addition, steam supply would add to the complexity of the system and would need on board storage. In the current model, the fuel was converted into carbon monoxide and hydrogen prior to the SOFC through partial oxidation. Partial oxidation is considered in this study because it makes use of air, which can be an advantage for mobile applications [26]. The reformer model aims at determining the amount of fuel in mol (mol_{fuel_FC}) and the heat energy required by the system, considering the stoichiometric reactions of the partial oxidation. The amount of fuel needed by the reformer is equivalent to the ratio of the P_{FC_in} and the specific calorific energy contained in the outlet stream of the reformer. These values are calculated using the LHVs of carbon monoxide and hydrogen as presented by equation (10). The required thermal energy corresponds to the sensible and latent heats of the concerned fuels and the enthalpy of formation.

$$mol_{fuel\_FC} = \frac{P_{FC\_in}}{n_{CO}\, LHV_{CO} + n_{H2}\, LHV_{H2}} \quad (10)$$

2.1.4 Fuel tank

The level of fuel inside the tank is monitored using a state of charge ($Tank_{SOC}$) presented as the ratio of the current level (*Fuel level*) and the maximum capacity ($Max_{Fuel\ level}$). The amount of fuel varies according to the need of the powertrain. To simplify the modelling, the quantity of fuel is first considered in moles and can later be converted in volume or pressure units according to the storage state of the fuel. A minimum storage level of 10% is introduced to comply with the shutdown process of the FC system in practice.

$$Tank\ soc = \frac{Fuel\ level}{Max_{Fuel\ level}} \quad (11)$$

2.2 SOFC control strategies

For the start-up, the SOFC stacks have to be heated to the nominal operating temperature (750 ^{o}C). A potential operation below this temperature (with a consequently smaller electrical power output and a related heat production) is not considered in the present study. For some applications, a faster heating is desired and therefore, two control options were designed, which are distinguished by the heating procedure. The basic option considers the complete heating of the SOFC module with all SOFC stacks before starting the operation and thus the electricity production. In the advanced option, the SOFC stacks in the module are started successively, i.e. a first stack is heated initially and the operation is started, which produces heat. This heat is utilized for heating the next stack in the module and so forth. Both options consider the same external heating power used by the basic control strategy, which is stopped once the overall module is heated. Figure 3 illustrates the general algorithm used for the advanced SOFC control strategy. This control option contains the five

operational modes described below. In order to represent the basic strategy, the SOFC module is considered as one stack only.

- Mode 0: SOFC off

The SOFC module and heating system are not activated.

- Mode 1: SOFC stacks warm up and start gradually – Low power output of the SOFC stacks

The heating system starts and the SOFC stacks are heated successively. Once a stack is operational, electricity is produced and the generated heat is redirected towards heating the remaining stacks. If the DoD of the battery is lower than 50%, the power generated by the stacks ($P_{SOFC\_mode\_1}$) is the average power demand of the vehicle reduced by a coefficient ($Level_{mode1}$), see equation (12).

$$P_{SOFC\_mode\_1} = Level_{mode1} * Power_{average} \ (if \ Level_{mode1} * Power_{average} < Nominal \ power \ stack \ activated) \quad (12)$$

In case the operating stacks cannot provide this power, they supply their nominal power as described by equation (13).

$$P_{SOFC\_mode\_1} = Nb\_stack_{activated} * Power_{nominal \ stack} \quad (13)$$

The number of activated stacks is calculated by equation (14), where $Q_{FC\_heating\_module}$ is the thermal energy being transferred to the module and $Q_{FC\_stack\_required}$ is the thermal energy required by each stack.

$$Nb\_stack_{activated} = \frac{Q_{FC\_heating\_module}}{Q_{FC\_stack\_required}} \quad (14)$$

- Mode 2: SOFC stacks start gradually – Max power output of the SOFC stacks

Mode 2 follows the same procedure as described in Mode 1 with the difference that the DoD of the battery reached 50%. The operating stacks provide their nominal power to support the powertrain. Equation (13) is applied for this mode.

- Mode 3: SOFC stacks completely heated– Nominal power output of the SOFC module

The heating system is stopped and the complete SOFC module is activated. If the DoD of the battery is higher than the predefined level (i.e. 5%), the power generated by the stacks is the nominal power of the module following equation (15).

$$P_{SOFC\_mode\_3} = Nb_{stack} * Power_{FC\_model} \quad (15)$$

- Mode 4: SOFC module completely heated – Reduced power output of the SOFC module

The heating system is stopped and the complete SOFC module is activated. If the DoD of the battery is lower than a predefined minimum level (i.e. DoD_mode4=5%), the SOFC module switches to a low power regime and follows the equation (12).

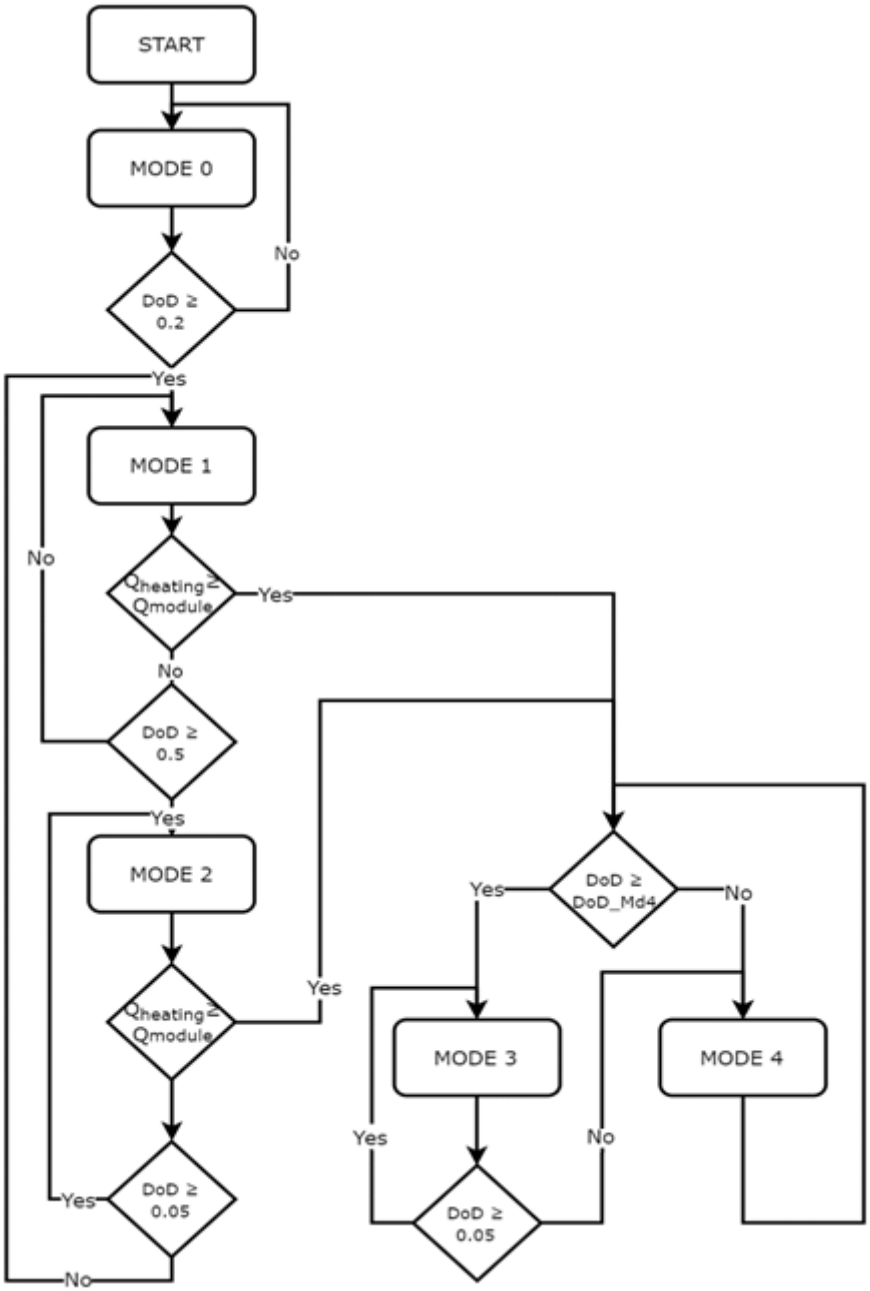

Figure 3 SOFC Module advanced control algorithm

2.3 Powertrain control management

In order to have the maximum efficiency of the system combining the battery pack, the fuel cell module and the electric engine, Alfonsin *et al.* [27] developed a logical flowsheet that contains the different interactions between each part of the vehicle's powertrain. The present study considers the same algorithm with the only difference that the fuel cell system works with two regimes instead of providing only the nominal power. The procedure uses a specific driving cycle and all the different parameters required for the model parts introduced in the previous sections as input. For the implementation of this algorithm, the MATLAB® scripts created with the submodules in the previous sections are combined and follow the algorithm illustrated in Figure 4.

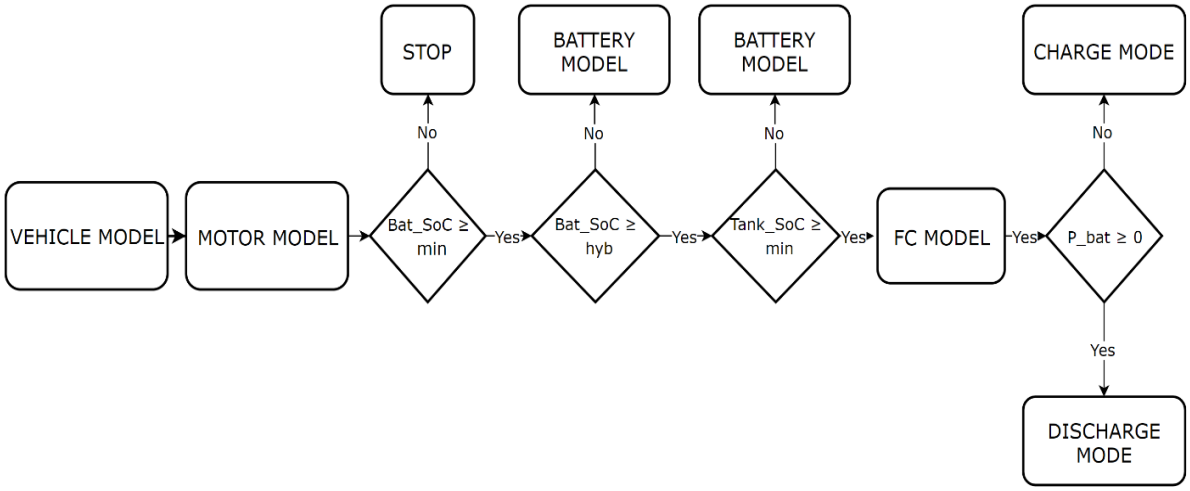

Figure 4 Powertrain control algorithm (from [27])

2.4 Simulation parameters

2.4.1 Driving cycles

The simulations make use of the "New European Driving Cycle" (NEDC) and the "Worldwide Harmonized Light Vehicles Test Procedure" (WLTP), displayed in Figure 5. Both are designed to mimic vehicles in urban environments. For verification purposes, the US06 driving cycle was also used ([28, 29]).

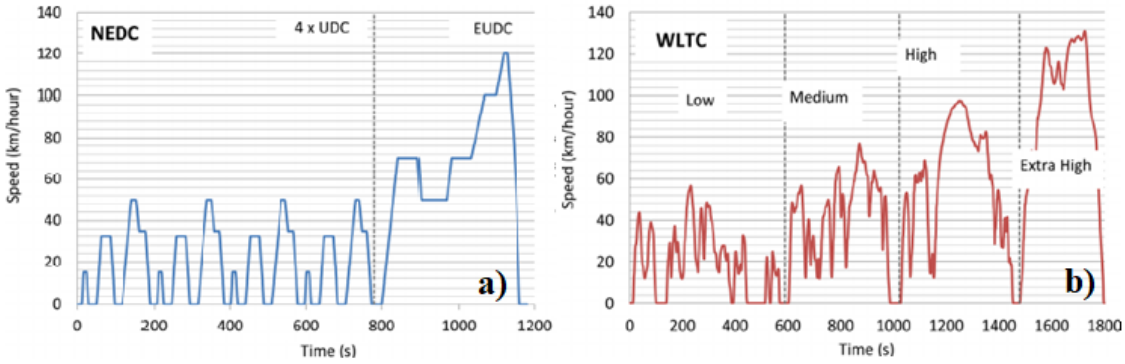

Figure 5 Speed profiles of NEDC (a) and WLTC (b) driving cycles, from ref. [29]

2.4.2 Model parameters

The WLTP driving cycle and the Nissan Leaf Acenta were used as reference case due to the accessibility of their technical specifications. The weight of the battery pack was estimated to 367 kg after a linear extrapolation from the data provided with the Nissan Leaf Visa [28]. The used parameters are listed in Table 3.

The FC heating time was set to 20 min for the simulations. This value is based on the targets defined for startup of SOFC APUs for trucks in the range of 15-30 min [30, 25].

Table 3. Reference configuration of the vehicle

Parameter	unit	Value
Charging time	[hour]	3
FC heating time	[hour]	0.33
Battery capacity reduction	[%]	50
FC control strategy	[-]	Basic or advanced
Tank volume	[l]	10
Fuel	[-]	LNG

Different configurations were simulated in order to investigate the performances of the system in a wide range of combinations of battery and SOFC for a given car and varying fuels. Table 4 lists the varied parameters.

Table 4. Parameter ranges for sensitivity analysis

Parameter	Unit	Range	Increment
Battery charging time	[hours]	0.5 - 3	0.5
FC heating time	[hours]	0.33 - 1	0.16
Battery capacity reduction	[%]	0 - 60	10
FC control strategy	[-]	Basic. Advanced	[-]
Tank volume	[l]	10-70	10
Fuel	[-]	CNG, LNG, LPG	[-]

All combinations of parameters in table 4 were simulated according to the algorithm shown in Figure 6.

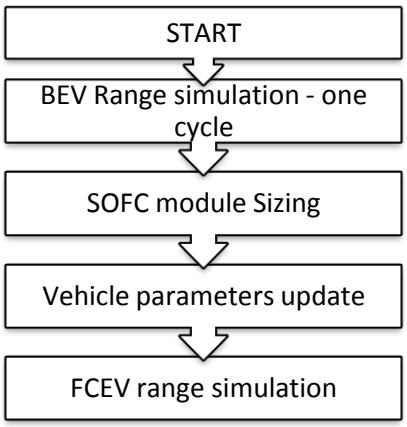

Figure 6 Overview over FCEV model analysis

3 Simulation results and discussion

3.1 Battery electrical vehicle model validation

The model was validated by considering a BEV (i.e. without an SOFC) where the simulated driving ranges can be compared to published data. For this validation only the vehicle dynamics, motor and battery scripts were considered. The Nissan Leaf Acenta and Nissan Leaf Visa were selected with a battery capacity of 30 kWh and 24 kWh, respectively. The WLTP and US06 driving cycles were used for the simulation. The reference parameters and performances were measured by the ADAC [2] and the U.S. Department of Energy National Laboratory [31]. For the model validation, the full battery capacity was assumed.

Figure 7 displays the simulation results of the electrical motor power (Figure 7a) and the current drained from the battery of the Nissan Leaf Visa (Figure 7b). The model considered the driving cycle US06 and an empty weight of 1474 kg. Both the model results and experimental measurements in this simulation appear to be in the same range with respectively a maximum cycle power of 91 kW against 89 kW and a drained current of 251.9 A against 255.3 A.

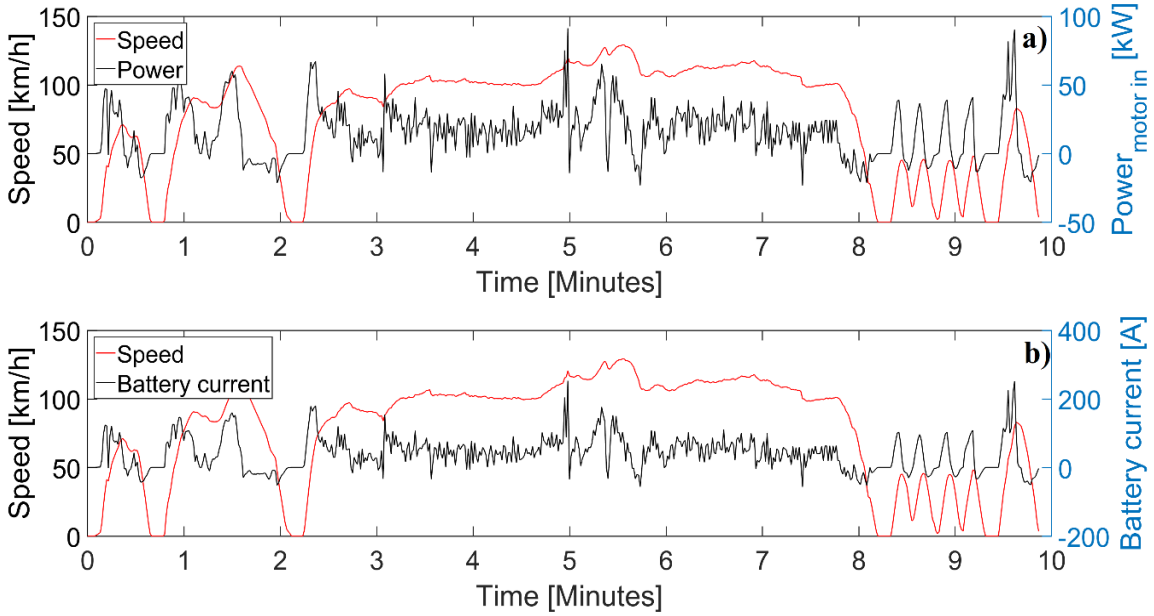

Figure 7 Simulation of battery current (a) and power (b) of a Nissan Leaf Visa using the US06 driving cycle

Figure 8 illustrates the results of a driving range simulation for the Nissan Acenta using the WLTP driving cycle. The OCV calculated by the model drops continuously from 400 to 350 V with recurrent peaks corresponding to the accelerations (Figure 8a). The DoD was set to 80% as maximum. With this limit, the obtained range at the end of the simulation is 156.3 km (Figure 8b) against 155 km as published [28]. The deviation of only 0.86% indicates the validity of the developed model. By applying the NEDC driving cycle to the same vehicle, a range of 177.8 km was obtained compared to 170 km stated by the manufacturer, which is still only a small deviation of 4.6%.

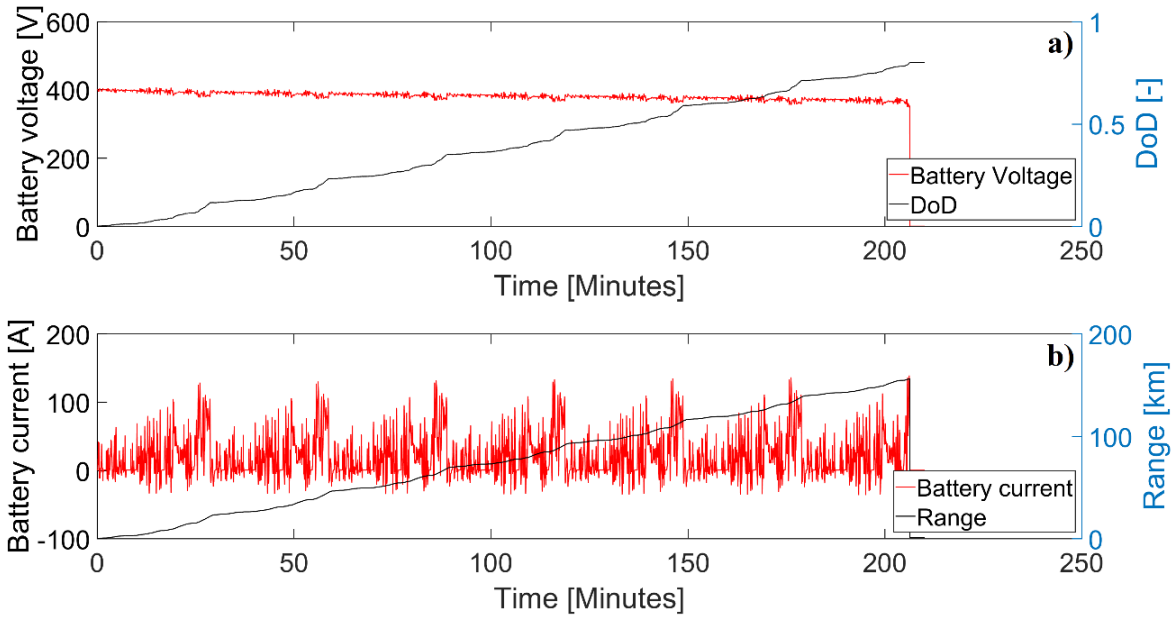

Figure 8 Simulation of the DoD (a) and range (b) of a Nissan Leaf Acenta using the NEDC driving cycle

The simulations were repeated for more BEVs. Even though some of the key parameters were not published and had to be estimated, a good agreement between simulated and published driving ranges was achieved, with deviations between 1 and 9%, only. With these results, the model was considered valid and was extended to include the SOFC module.

3.2 SOFC/BEV simulation

After validation, the model was applied to a SOFC/BEV by reducing the battery capacity of the reference case by 50% and by integrating the SOFC module with the fuels CNG, LNG, or LPG. Target parameters were driving ranges and energy consumptions of the hybrid vehicles. Afterwards, selected model parameters were varied in order to study impacts of for example battery capacity, tank volume or SOFC power density.

3.2.1 Technology comparison

For the technology comparison of ICE vehicles, BEVs, and SOFC/BEVs, the tank volume was changed to 30 l (instead of 10 l, see Table 3) in order to represent better a standard tank size in an ICE vehicle. The larger tank volume affects other parameters as well. The SOFC module was adjusted to 12 kW for LPG, LNG and CNG, considering the NEDC driving cycle. The new weights of the vehicle are 1460 kg, 1459 kg and 1456 kg, respectively. Start & stop patterns were not included in the simulation. Figure 9 presents the driving ranges of selected vehicles based on published data together with the results of the model in this work.

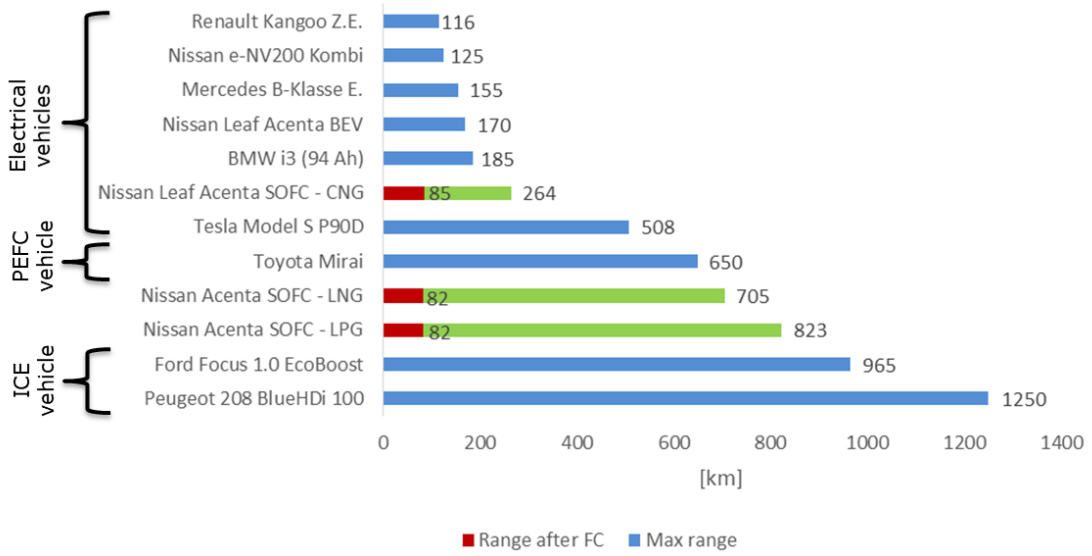

Figure 9 Driving ranges of ICE vehicles and BEVs (blue columns, refs. [32, 33]), SOFC/BEVs simulated by the model in the present work (green columns), range after FC is the remaining battery range after using up the SOFC fuel (red columns)

The longest driving ranges are naturally achieved by the ICE vehicles (Ford Focus, Peugeot 208 in Figure 9), followed by the Toyota Mirai, (PEFC-battery hybrid) and the Tesla Model S, which is the BEV with the longest driving range among present BEVs (see Figure 9).

When integrating an SOFC into a BEV, the driving ranges increase substantially, in particular when using LNG and LPG fuel. The integration of an SOFC into the Nissan Acenta increases the range by factors of 4-5 (even though the battery capacity was reduced by 50%) and even passes the best PEFC car and all BEVs. Also, when using CNG fuel, the range increased significantly by about 100 km, which is longer than most of the BEVs of this ranking, with the exception of the Tesla Model S. After the fuel has been used and the SOFC stopped operating, the battery could support the vehicle for an additional distance of around 80 km before reaching 80% of DoD (see Figure 9).

Apart from the driving range, also the total energy consumption is an important factor. The results of the simulation in this work are compared to published values in Figure 10. The SOFC/BEVs have slightly higher total energy consumptions as purely BEVs. This is due to the concept used in the present model. The battery capacity is reduced to 50% compared to the BEV reference and the vehicle runs mainly with the SOFC activated, which has to charge the battery and support the powertrain simultaneously. This behaviour is more pronounced considering LNG with a resulting energy consumption of 23 kWh/100 km compared to the 14 kWh/100 km of the Nissan Leaf Accenta BEV. These results are still comparable to the Toyota Mirai that consumes 25 kWh/100 km according to the manufacturer [28]. Finally, all SOFC/BEV combinations are significantly below ICE vehicles (see Figure 10).

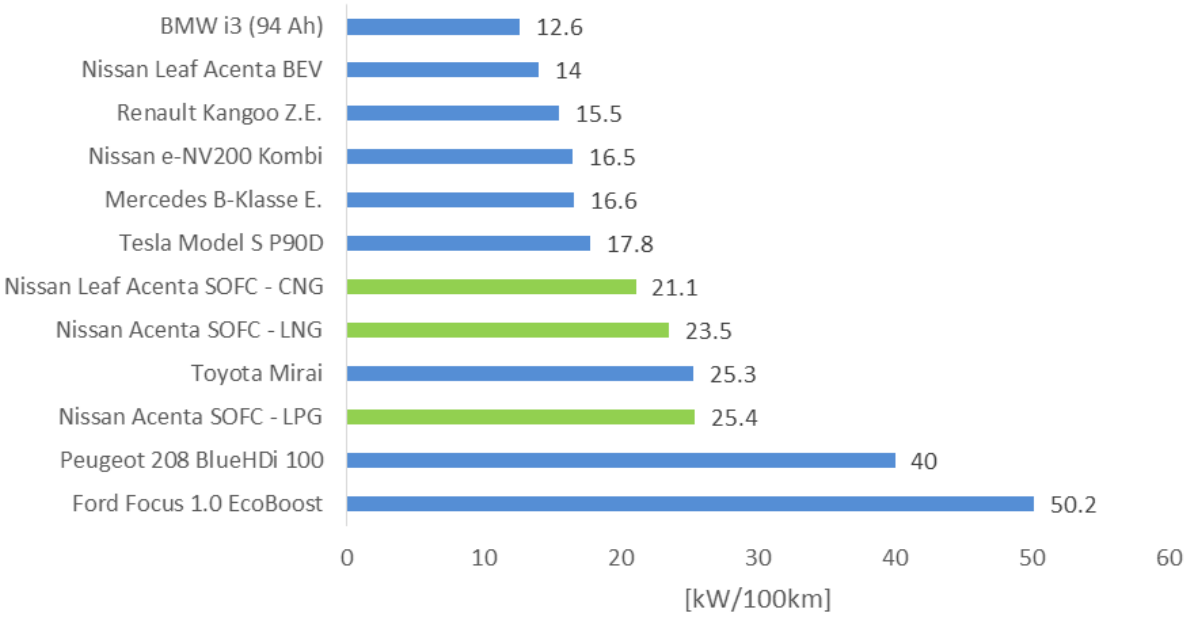

Figure 10 Energy consumptions of ICE vehicles and BEVs (blue columns, refs. [32, 33]) and SOFC/BEVs simulated by the model in the present work (green columns)

The comparison between the ICE vehicle, BEV, PEFC/BEV and SOFC/BEV technologies shows that the concept of a hybrid of SOFC and battery gives a good compromise in terms of driving range and energy consumptions. It thus combines the attractive user convenience, considering

charging time and fuel availability, in addition to the environmental benefits in the parameter space of this study.

The user benefits from the existing fuel infrastructure, which also saves substantial investment costs, from the fast fuelling times related to gaseous/liquid fuels, and from the long driving ranges that approach those of the ICE vehicles. On the other hand, the smaller energy consumption of the SOFC/BEV concept regarding the applied driving pattern can significantly reduce the CO_2 emissions as compared to ICE vehicles. Together with the prospect of developing technologies to produce CNG, LNG, and LPG using renewable sources (such as Power-to-gas or Power-to-liquid, [34]), the CO_2 footprint and environmental impact from SOFC/BEVs could be reduced even further.

3.2.1 Fuel cell module control strategies

After the general technology comparison, the SOFC/BEV concept was further analysed regarding control strategies and parameter variations. Two strategies were considered for the SOFC start-up in the simulations. In the first one, all stacks of the SOFC module are heated to operating temperature and afterwards started. In the second one, the stacks are heated successively and started as soon as one has reached operating temperature. In that way, the heat produced by one operating SOFC stack is used for heating the remaining stacks.

Figure 11 shows the first strategy. When the DoD of the battery has increased above 20%, the SOFC systems starts with the mode 1 by burning the fuel to heat up the SOFC module. At operating temperature, the module switches to mode 3 and provides its nominal power. At the same time, the fuel flow rate is reduced slightly to provide the needed fuel for the electrochemical processes. The battery is simultaneously charged and oscillates between 5% and 10% of DoD until the tank level is below 10%, which activates mode 0 and stops the SOFC system. From this point the vehicle operates only on BEV mode.

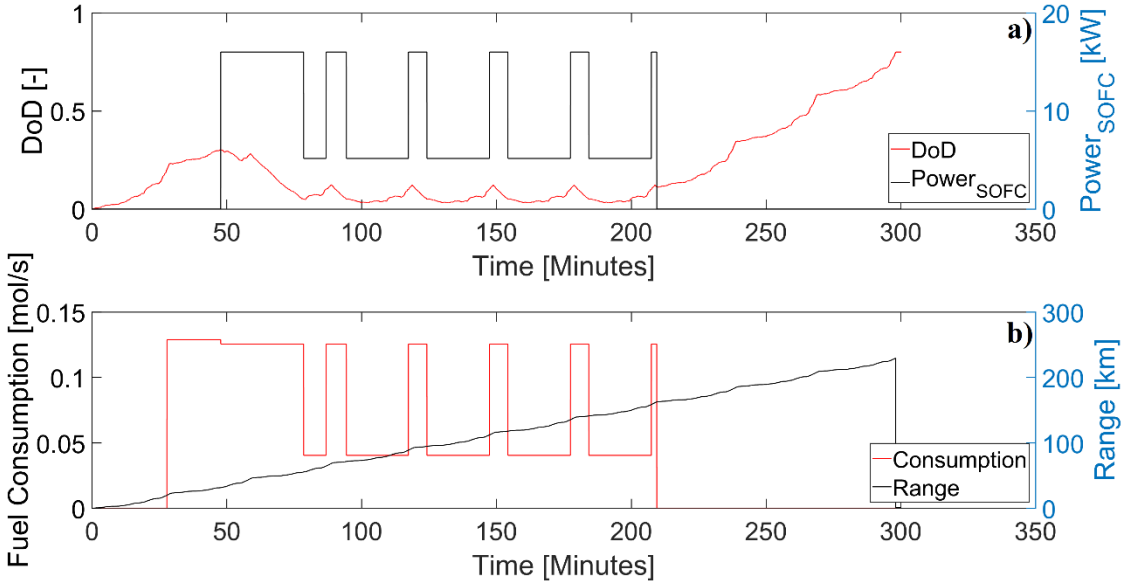

Figure 11 DoD of the battery and SOFC power (a) and fuel consumption and driving range (b) for the basic SOFC control strategy

This basic control strategy was compared to the advanced control strategy. The major difference is in the heating phase. The heating starts again after 20% of DoD of the battery. The stacks are successively started (steps in Figure 12). The produced power and heat are transferred to the rest of the system. After heating of the complete SOFC module the stacks provide their nominal power as described in the basic control strategy.

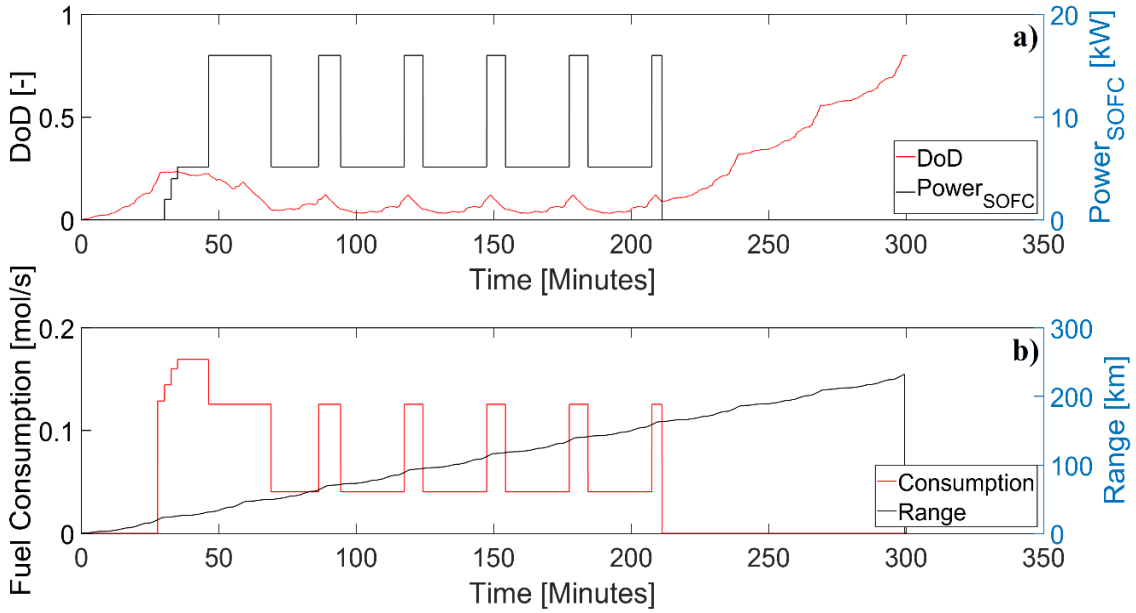

Figure 12 DoD of the battery and SOFC power (a) and fuel consumption and driving range (b) for the advanced SOFC control strategy

The basic control strategy requires 20 minutes heating time, as it was pre-set for the simulation (see Table 3). By using the advanced control strategy, this time can be reduced by 1.5 min, i.e. a slightly faster SOFC start-up is achieved. Furthermore, 18% of the usable fuel was used by the basic control strategy, while it was 16.7% for the advanced control strategy, assuming a fuel tank containing 10 litre of LNG and 10% as lower filling limit. These values indicate a small positive impact on the SOFC start-up in terms of speed and fuel consumption when applying the successive start of SOFC stacks within the frame conditions given in the present study. By improving the advanced control strategy even more, the advantage could be further increased and might lead to a reduction of the needed battery capacity.

3.2. Battery capacity

The battery capacity is a critical parameter for BEVs because it directly affects the range, weight, and manufacturing costs. In the present study, the battery supplies the energy to the powertrain when the SOFC module is not operational. It is therefore interesting to assess the performances of the vehicle when successively reducing the size of the battery.

In Figure 13, the driving ranges when reducing the battery sizes are depicted for the three fuels. The SOFC module was kept at the same power level. Clearly, a battery reduction leads to a decrease of the driving range and thus also the remaining range after usage of the fuel for the SOFC. This reduction is largest when using CNG fuel (ca. 70 km when reducing the battery capacity by 60%, see Figure 13) and smaller when using LNG and LPG (ca. 55 km when reducing the battery capacity by 60%, see Figure 13). The simulation also shows that the possible driving range reduction does not scale 1:1 with the battery capacity reduction. The driving range is less affected by the battery reduction due the energy provided by the fuel cell module, which would favour a decision for reducing the battery. The driving range could then be increased by adjusting the SOFC module size or the volume of the fuel tank (see next section).

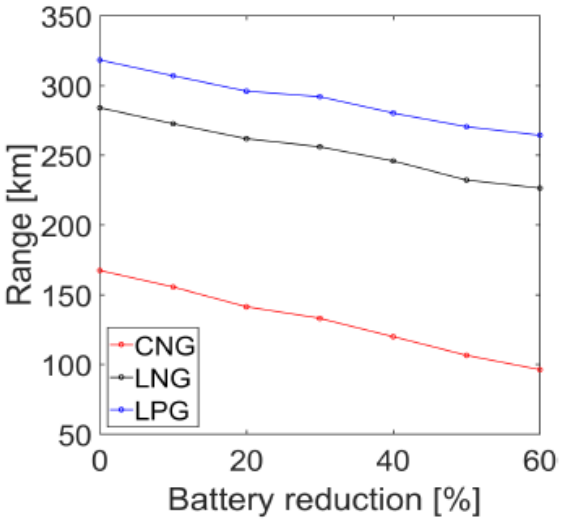

Figure 13. Effect of reducing the battery capacity on the driving range of the SOFC/BEV using the Nissan Leaf Acenta and a 10 l tank

3.3 Fuel tank volume

In order to adjust driving ranges, changing the fuel tank volume is corresponding to a change of the battery capacity, as the energy is contained in the fuel in case of the SOFC and in the battery material in case of the BEV. Increasing the battery capacity leads to a large increase of both weight and costs, in contrast to an increase of the fuel tank.

Increasing the size of the fuel tank increases the driving range linearly (Figure 14a). The impact of the tank volume is thus significant. The increase of the tank volume also increases the energy consumption of the vehicle to a certain extent (Figure 14b). This increase is less when approaching larger tank volumes and is minor as compared to the increase of driving range (Figure 14a). The slight increase can be explained by the SOFC control strategies. The SOFC system used has five working modes from 0 to 4 during the simulation. The lowest energy consumption of the vehicle is in mode 0 when the SOFC system is in standby, while the highest consumption level is related to the nominal power of the system in mode 3. Increasing the volume of the fuel tank also increases the periods in mode 3, which overall leads to a slightly larger energy consumption pattern.

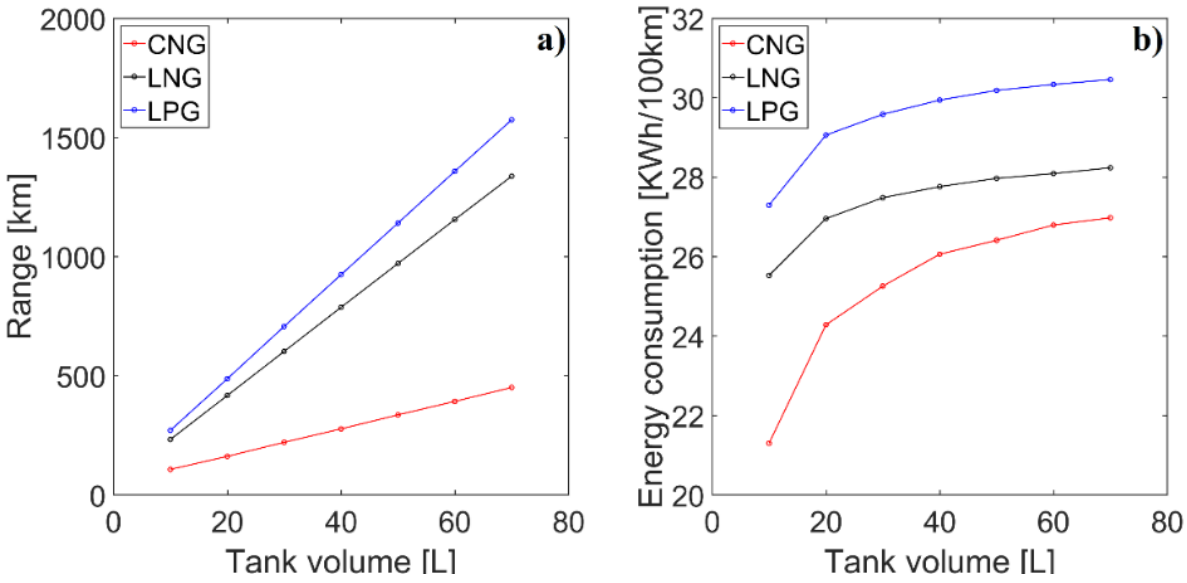

Figure 14 Effect of tank volume on driving range (a) and energy consumption (b) of the SOFC integrated into a Nissan Leaf Acenta battery vehicle, reference configuration and WLTP driving cycle

3.4 Fuel cell module power density

The performance of the SOFC module and thus the SOFC/BEV greatly depends on the power output of the specific stack. For the present study, a commercially available SOFC stack was modelled [22]. As the SOFC technology is under rapid development, more active stacks with smaller area specific resistances and higher power output per area/volume/weight can be expected to become available. It is thus interesting, how much the performance of a SOFC/BEV would be affected by improvements of the core SOFC technology.

Figure 15 illustrates how the improvement of performance of the SOFC stack used in this study expressed by a power density coefficient would affect the number of SOFC stacks required, the heating time, and the driving range. The number of stacks required for the SOFC module could be reduced from eight to five when increasing the power density of the current reference stack by 50%. This is a significant number with large cost reduction potential. At the same time, the amount of fuel required for heating the system could be reduced by 6% due to the reduced thermal mass (Figure 15a). Furthermore, the heating time for starting the SOFC operation could be reduced by 0.5 min and the driving range increased by 18 km (8%, Figure 15b). For these results, a 10 liters tank (see Table 3) was used.

When increasing the tank volume to 30 liters, the improvements would become even more distinct. The Nissan Leaf weight could be reduced by 54 kg due to the shorter stacks, the total range could be increased by 27 km and the fuel consumption for the SOFC heating step could be reduced by 3.4%. In addition to this effect, the volume of the system would also be positively affected.

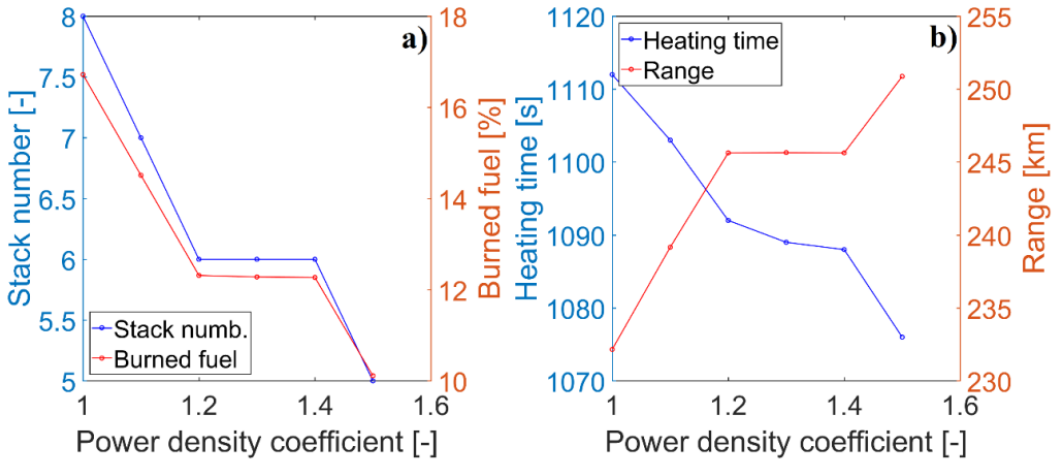

Figure 15 Effect of the SOFC stack power density as compared to the commercial SOFC stack reference on the stack number for the needed SOFC power and burned fuel for heating (a) and on the heating time and driving range (b)

3.5 Fuel comparison

From the introduction, the availability of the fuels of interest in this work was already presented (see Table 1). LPG is clearly the best available of the three fuels, almost as well-established as petrol with a station density by only a factor of about two smaller, followed by CNG and LNG. LNG is certainly expected to increase in importance considering the recent power-to-X concepts which are based on using electricity from renewable sources [34].

Figure 16 depicts the heat flows in the fuel reformer and SOFC system and the driving ranges depending on the type of fuel with a 10 liters tank. In terms of range, LPG followed by LNG provides the best values with 270 km and 230 km, respectively (Figure 16a). With CNG fuel 106 km can be achieved. Note that for these simulations different parameters (those from Table 3) were used than for the technology comparison in Figure 9. The poorer performance of the CNG is primarily due to the low energy content in the tank with 10 liters volume and 200 bars at ambient temperature. Moreover, this range is smaller than the original vehicle; this is because the battery capacity was reduced by 50% and an SOFC module integrated. More specifically, 54% of the CNG contained in the tank is used to warm up the SOFC stacks while the other fuels can support the powertrain for a longer period, because less fuel is needed for the initial stack heating.

With the partial oxidation as reformer technology and considering stoichiometric reactions, it appears that in case of the CNG and LNG an additional heating power of up to 4 kW is required to complete the reforming process. These values include the heating and evaporation of the fuel streams entering the reformer combined with the thermal energy production during the reaction. Using LPG, the heat generated by the reforming reaction is already sufficient to support the reactions, which is clearly an advantage of this fuel (Figure 16b).

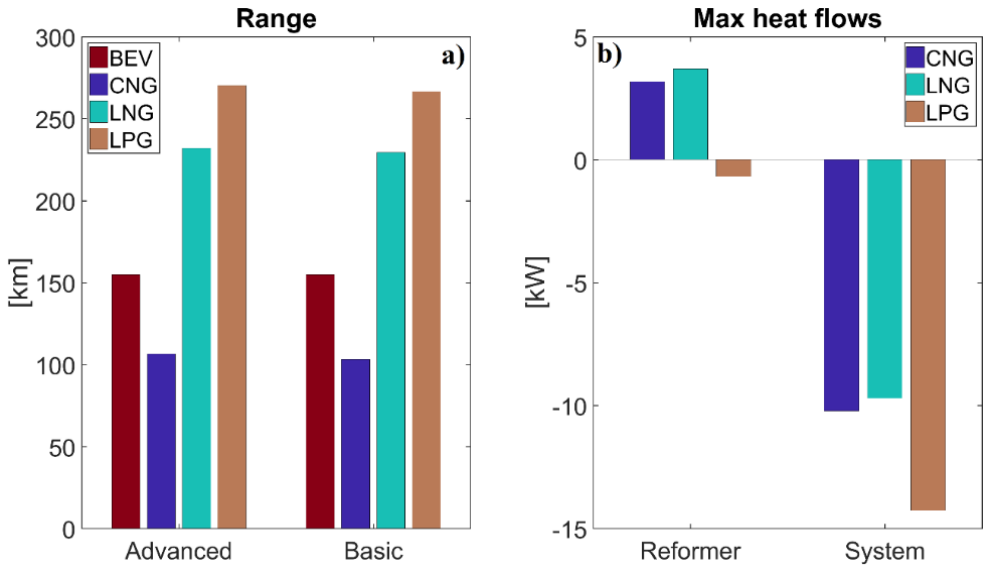

Figure 16 Driving ranges (a) and system heat balance (b) for different fuel options

For the current study, the partial oxidation was selected as pre-treatment of the fuel to avoid the additional use of water for the process. Using this option, about 16% of a 10 liters fuel tank is required to preheat the SOFC module for a period of 20 minutes for the example of a Nissan Leaf type SOFC/BEV. The fuel consumption for the heating step of the SOFC module in combination with a realistic driving pattern of light vehicles in urban areas means that most of the available volume would be used for the start-up part, leaving less time to recharge the battery. Therefore, the SOFC/BEV concept seems to be more suited for long driving range vehicles such as buses, trucks or trains. Those transportation options usually drive several hundred kilometers without long period stops. They would better fit the technological constraints of SOFCs and avoid several heating steps during operation. Another possibility could be to allow the fuel cell system to charge the battery even when the vehicle is not in operation. In this case, the state of charge of the battery would be the main factor determining the operating conditions of the SOFC module and could be applied for light vehicles as well.

4. Conclusions

An SOFC/BEV concept was designed and implemented into a computer model. The aim was to show that the presented concept could overcome current challenges with BEVs and PEFC/BEVs. These challenges are short driving ranges, long fuelling times, insufficient charging and fuelling infrastructure, and high costs. The concept can still take advantage of high efficiencies inherent in batteries and PEFCs and combine those with long driving ranges and fast fuelling utilizing the existing fuelling infrastructure.

An SOFC/BEV model was successfully established and validated using standard driving cycle data from BEVs. A comparison of the driving ranges with BEVs, ICE vehicles and a PEFC/BEV demonstrated the benefits of an SOFC/BEV concept. The longest driving ranges among the electric vehicles were obtained; they were even close to the performances of ICE vehicles, which would exhibit a great benefit for the SOFC/BEV car users. Furthermore, the energy consumption was

comparable to the Toyota Mira with a PEFC/BEV concept. The energy consumption was slightly higher than that for pure BEVs. Compared to ICE vehicles, the energy consumption was much lower for SOFC/BEVs. Thus, the user comfort, cost reduction (e.g., usability of existing infrastructure), and environmental impact (considering CO_2 and NO_x emissions) are in favor of the concept presented in this work. The benefits appear more significant for a constant operation concept, for example bus and train transport or continuous SOFC/BEV operation.

SOFC operating temperatures are in the range of 700-800 ^{o}C, which is sometimes considered a disadvantage for applications in the transport sector. A part of this potential disadvantage can be overcome by using the SOFC/BEV battery to heat the SOFC module. Two control strategies were proposed and compared. The simulation results showed that by successive heating and starting of operation of the SOFC stacks and thus providing heat to the remaining stack, the heating (start-up) time of the SOFC module decreased. At the same time saving of fuel is possible.

To increase the driving range, a combination of battery reduction and fuel tank volume increase was studied to take advantage of the resulting lower manufacturing costs (battery materials against fuel tank costs), the weight reduction and the increase of useable space in the vehicle's powertrain. The simulation results demonstrate that the driving range is reduced when the battery capacity is reduced, as expected because the SOFC was not adjusted, which affects the flexibility of short range applications. In addition to the power required for the vehicle during heat up of the SOFC stack, the battery also provides the energy for the peak accelerations before being recharged by the SOFC module, which has to be considered when optimizing the overall system. The increase of the fuel tank volume to from 10 to 30 liters significantly increased the driving range to the values of a standard ICE vehicle.

The study showed that an improvement of the SOFC technology in terms of power output is a significant parameter to decrease costs and increase driving ranges.

Among the considered fuels, LPG and LNG offer competitive performances compared to petrol and diesel. CNG provides results, which are still better, i.e. longer driving ranges, than pure BEVs.

References

1 S. Kukkonen, „Energy consumption analysis of battery electric vehicles in underground environments", Underground Mining Technology 2017 – M Hudyma & Y Potvin (eds) © 2017 Australian Centre for Geomechanics, Perth, ISBN 978-0-9924810-7-0.

2 ADAC, "Auto-Test: Finden Sie Ihr Wunschauto." [Online]. Available: https://www.adac.de/infotestrat/tests/auto-test/default.aspx. [Accessed: 11-Sep-2017].

3 Battelle Memorial Institute, "Manufacturing Cost Analysis of 100 and 250 kW Fuel Cell Systems for Primary Power and Combined Heat and Power Applications", U.S. Dep. Energy, 2016.

4 U. Bossel, "Solid oxide fuel cells for transportation", J. KONES Internal Combustion Engines, vol. 12, 3-4, 2005.

5 J. Rechberger, A. Kaupert, J. Hagerskans, and L. Blum, "ScienceDirect Demonstration of the first European SOFC APU on a heavy duty truck", Transp. Res. Procedia, vol. 14, pp. 3676–3685, 2016.

6 P. Agnolucci, "Prospects of fuel cell auxiliary power units in the civil markets", Int. J. Hydrogen Energy, vol. 32, 4306 – 4318, 2007.

7 N. Briguglio, L. Andaloro, M. Ferraro, and V. Antonucci “Fuel Cell Hybrid Electric Vehicles”, Open access peer-reviewed chapter, DOI: 10.5772/18634.

8 Nissan, Fuel Cells Bulletin Volume 2016, Issue 7 (2016) 2-3: https://doi.org/10.1016/S1464-2859(16)30165-1.

9 Battelle Memorial Institute, “Manufacturing Cost Analysis of 100 and 250 kW Fuel Cell Systems for Primary Power and Combined Heat and Power Applications”, U.S. Dep. Energy, 2016, pp. 128.

10 KELAG-Kärntner Elektrizitäts-Aktiengesellschaft, “- EV-Charging Stations in Europe - ev-charging.com,” 2017. [Online]. Available: https://ev-charging.com/at/en/info/statistics. [Accessed: 02-Oct-2017].

11 AEGPL, “AEGPL - LPG stations in Europe.” [Online]. Available: http://www.aegpl.eu/lpg-stations-in-europe.aspx. [Accessed: 02-Oct-2017].

12 NGVA, “STATISTICAL REPORT 2017,” pp. 1–12, 2017.

13 NGVA Europe, “NGVA Europe - Search nearby / by country.” [Online]. Available: https://www.ngva.eu/search-nearby-by-country. [Accessed: 02-Oct-2017].

14 W. James, “An Introduction to SAE Hydrogen Fueling Standardization”, *U. Dep. Energy*, 2014.

15 T. & M. Council, “Future Alternative Fuel Engine Paper (2001)—1”, no. March 2001, 2001.

16 “A Feasibility Study of Natural Gas Vehicle Conversion In Wyoming Public School Districts”, 2012.

17 J. Larminie and J. Lowry, Electric Vehicle Technology Explained. Chichester, UK: John Wiley & Sons, Ltd, 2003.

18 K. Young, C. Wang, L. Y. Wang, and K. Strunz., Electric Vehicle Integration into Modern Power Networks. 2013.

19 C. Zhang, J. Jiang, L. Zhang, S. Liu, L. Wang, and P. C. Loh, A generalized SOC-OCV model for lithium-ion batteries and the SOC estimation for LNMCO battery. Multidiscip. Digit. Publ. Institute- Energies, 2016.

20 J. Li, S. Zhou, and Y. Han, “Event-Based Modeling for Battery Manufacturing Systems Using Sensor Data”, Adv. Batter. Manuf. Serv. Manag. Syst., pp. 57–78, 2017.

21 J. V. Barreras, E. Schaltz, S. J. Andreasen, and T. Minko, Datasheet based modeling of Li-Ion batteries. IEEE Vehicle Power and Propulsion Conference, VPPC, 2012.

22 L. Ningbo SOFCMAN Energy Technology Co., SOFCMAN. [Online]. [Online]. Available: http://www.sofcman.com/stack1.html. [Accessed: 05-Oct-2017].

23 M. Halinen, M. Rautanen, J. Saarinen, J. Pennanen, A. Pohjoranta, J. Kiviaho M. Pastula, B. Nuttall, C. Rankin, B. Borglum, “Performance of a 10 kW SOFC Demonstration Unit.”, ECS Trans., vol. 35, no. 1, pp. 113–120, 2011.

24 W. Huang, S. Gopalan, U. B. Pal, and S. N. Basu, “Oxidation Studies on Crofer 22 APU Alloy Under Simulated SOFC Operating Conditions.”, ECS Transactions, vol. 7, no. 1, pp. 2379–2384, 2007.

25 J. Rechberger, project coordinator, project report of “Demonstration of 1st European SOFC Truck APU”, DESTA project, http://www.desta-

project.eu/fileadmin/downloads/Deliverables/278899_DESTA_Final_Publishable_Summary_Report.pdf [Accessed: 09-Nov-2018].

26 A. Rabbani and M. Rokni, “Modeling and Analysis of Transport Processes and Efficiency of Combined SOFC and PEMFC Systems”, Energies 2014, 7, 5502-5522; doi:10.3390/en7095502.

27 B. Alfonsin, R. Maceiras, A. Cancela, and A. Sanchez, “Modelization and Simulation of an Electric and Fuel Cell Hybrid Vehicle under Real Conditions”, Eur. J. Sustain. Dev., vol. 4, no. 2, pp. 135–140, 2015.

28 T. Gray Jeffrey Wishart and M. Shirk, “2011 Nissan Leaf VIN 0356 Electric Vehicle Battery Test Results.”, no. VEHICLE TECHNOLOGIES PROGRAM, 2016.

29 A. Marotta, J. Pavlovic, B. Ciuffo, S. Serra, and G. Fontaras, “Gaseous Emissions from Light-Duty Vehicles: Moving from NEDC to the New WLTP Test Procedure.”, Environ. Sci. Technol., vol. 49, no. 14, pp. 83158322, 2015.

30 S. Shaffer, “Solid Oxide Fuel Cell Development for Auxiliary Power in Heavy Duty Vehicle Applications”, DOE Hydrogen Program, FY 2008 Annual Progress Report, https://www.hydrogen.energy.gov/pdfs/progress08/v_i_3_shaffer.pdf [Accessed: 09-Nov-2018].

31 T. Gray Jeffrey Wishart and M. Shirk, “2011 Nissan Leaf VIN 0356 Electric Vehicle Battery Test Results,” no. VEHICLE TECHNOLOGIES PROGRAM, 2016.

32 ADAC, “Peugeot iOn,” Autotest, 2009.

33 “The MIRAI Life Cycle Assessment Report,” ISO, vol. 14040, no. 14044, 2006.

34 M. Lehner, R. Tichler, H. Steinmüller, M. Koppe, M., “Power-to-Gas: Technology and Business Models”, SPRINGER, 2014.